

Presentation and use of a reactive transport code in porous media

Ph. Montarnal^{a,*}, C. Mügler^a, J. Colin^a, M. Descostes^a, A. Dimier^b, E. Jacquot^b

^a *Commissariat à l'Energie Atomique, Centre de Saclay, 91191 Gif-sur-Yvette Cedex, France*

^b *Agence Nationale pour la gestion des Déchets Radioactifs, 1-7 rue Jean Monnet, 92298 Châtenay-Malabry Cedex, France*

Received 19 April 2005; received in revised form 20 January 2006; accepted 28 January 2006

Available online 27 October 2006

Abstract

The safety assessment of nuclear waste disposals requires an accurate prediction of the radionuclides and chemical species migration through engineered barriers and geological media. It is therefore necessary to develop and assess qualified and validated tools which integrate both the transport mechanisms through the geological media and the chemical mechanisms governing the mobility of radionuclides. Such a reactive transport simulation tool has been developed in the context of the numerical software platform ALLIANCES. Different component codes are available: PHREEQC and CHESS for the chemical part, CAST3M, MT3D and TRACES for the transport part. A coupling scheme has already been implemented, qualified and validated on numerous configurations involving aqueous speciation, dissolution–precipitation, sorption and surface complexation.

Presently, the reactive transport numerical tool is used to simulate realistic configurations. This paper presents two of such applications: the migration of uranium in a soil with various redox conditions and the modelling of clay–cement interactions.

© 2006 Elsevier Ltd. All rights reserved.

Keywords: Reactive transport; Modelling; Uranium migration; Clay–cement interaction

1. Introduction

According to a law adopted by the French parliament in 1991, the French Nuclear Agency (CEA) and the French Agency in charge of the Management of Radioactive Waste (ANDRA) are responsible for the disposal and storage of nuclear waste and spent nuclear fuel in France. Various configurations of nuclear waste storage in deep geological formations have been studied since the law was adopted. In the near-field of a high-level radioactive waste (HLW) repository, coupled thermo-hydro-mechanical and chemical (T-H-M-C) processes will occur, involving processes such as heat generation and transport (due to radioactive decay of nuclear waste), infiltration of groundwater (hydrogeological processes), swelling pressure of buffer material due to saturation (mechanical processes) and chemical evolution of buffer material and porewater (chem-

ical processes). Laboratory and *in situ* experiments give access to short term evolutions. Natural analogue investigations give valuable informations for geochemical scenarios. Numerical simulation is required to quantify potential radioactive releases in a real situation. Therefore CEA, ANDRA and EDF are jointly developing the software platform ALLIANCES whose aim is to produce a tool for the simulation of nuclear waste storage and disposal repository. The goal of ALLIANCES (Montarnal et al., 2006) is to provide a working environment for the simulation and analysis of phenomena that must be taken into account for waste storage and disposal studies. ALLIANCES aim is not to develop a new scientific calculation code but a way to gather within the same simulation environment the already acquired knowledge and to gradually integrate the new one.

This paper presents the development and demonstration of the hydrogeochemical transport tool included in ALLIANCES. It is based on operator splitting and solves iteratively a geochemical model and a transport model. After a brief description of the physical and numerical

* Corresponding author. Tel.: +33 1 69 08 25 75; fax: +33 1 69 08 52 42.
E-mail address: philippe.montarnal@cea.fr (Ph. Montarnal).

models and of their validation, we focus here on two applications of the code. The first one deals with the migration of uranium in a soil with various redox conditions. The second one deals with the modelling of clay–cement interactions in the context of a waste repository.

2. The coupled reactive transport code

2.1. General model

The reactive transport model describes the spatial and temporal evolution of a set of chemical species that are, on the one hand, submitted to transport phenomena and, on the other hand, submitted to chemical reactions. Involved transport phenomena can be convection, diffusion and dispersion in porous media. Chemical reactions may be at equilibrium state or controlled by kinetics, in liquid, solid or sorbed phases. More precisely, heterogeneous reactions that exchange matter between the liquid and the solid phases are taken into account in addition to the usual homogeneous reactions occurring in the liquid phase such as aqueous complex formation, acid–base and redox reactions. The main heterogeneous reactions considered here are precipitation–dissolution of minerals and sorption such as cation exchange. In our applications, the chemical processes are usually faster than the characteristic times of the transport, so we may assume as a general rule that the chemical system has reached its thermodynamic equilibrium state. Only some precipitation–dissolution processes are assumed to be kinetically controlled.

The corresponding physical model is made of a set of partial differential equations describing species transport in liquid phase, and a set of non linear algebraic-differential equations corresponding to the chemical reactions that model species interactions.

2.2. Geochemistry

Chemical equations are presented in Mügler et al. (2004). We only describe here the main features of these equations. Transport equation is only solved for so called component species, representing a linearly independent basis of chemical entities so that every species can be uniquely represented as a combination of those components, and no component can be represented by another component than itself (Yeh and Tripathi, 1989). Non-component aqueous species are called aqueous secondary species. Their concentrations are obtained from aqueous equilibrium reactions involving the components as reactants. All equilibrium equations are based on the mass action law. Precipitation–dissolution reactions can be at equilibrium or kinetically controlled. Equations for adsorption equilibrium are obtained using the law of action mass in the same way as the aqueous equilibrium reactions on sorbed secondary species.

The code relies on the libraries of two geochemical codes solving the complex set of reacting chemical species:

CHESS, developed by CIG (France) (van der Lee and de Windt, 2002) and PHREEQC, developed by USGS (US) (Parkhurst and Appelo, 1999).

2.3. Hydrogeological transport

Hydrogeological processes involved are the transport by convection, dispersion and/or diffusion in 1D/2D/3D on structured and unstructured meshes. The transport of solutes is described by a set of partial derivative equations based on the principle of mass conservation. The transport equation of the j th component species in aqueous phase is written as follows:

$$\omega \frac{\partial c_j}{\partial t} - \nabla \cdot (D \nabla c_j - c_j u) = Q_j + R_j,$$

where ω is the porous media porosity, supposed constant, c_j the concentration of the j th aqueous component species, D , the diffusion–dispersion tensor, u , the Darcy velocity, R_j , a source term corresponding to chemical reactions and Q_j another source term. Transport coefficients are assumed the same for all species.

The Darcy velocity u is modelled by the Darcy equation in the stationary state:

$$\begin{cases} \nabla \cdot u = 0 \\ u = -K \nabla h, \end{cases}$$

where h is the hydraulic head and K the permeability tensor.

Several codes are available to simulate hydraulic flow and transport:

- CAST3M, developed by CEA (France): EFMH or VF schemes, GMRES or Bi-CGStab linear solvers, 2D/3D unstructured meshes (Dabbene, 1998; Bernard-Michel et al., 2003).
- Modflow/MT3D, developed by U. Alabama (US): VF scheme, GCG linear solver, 2D/3D structured meshes (Zheng and Wang, 1998).

2.4. The coupling algorithm

The coupling algorithm is sequential iterative (Yeh and Tripathi, 1989): at each time step the transport equation and the chemical equation are solved successively and iteratively until convergence (Mügler et al., 2004).

3. Validation of the coupled reactive transport code

In a first step, several analytical test-cases have been defined and used to validate the reactive transport code. Numerical results have been compared to analytical solutions. In order to validate the coupling model, all studied configurations necessarily involve exchanges between species in aqueous phases and in immobile phases (dissolution–precipitation or sorption phenomena). For example, we have simulated the diffusion of alkaline water in quartz

sand, leading to acid/base reactions simultaneous with mineral dissolution: quartz reacts with hydroxyl ions and dissolves. Numerical results for the spatial and temporal evolution of pH and Na^+ concentration have been successfully compared to analytical solutions, in 1D and 2D geometry (Mügler et al., 2004). Another test-case involves the dissolution of concrete by a carbonated groundwater, in a 1D geometry. It is a typical coupling problem that can be found near a waste disposal. In this configuration taken from Read and Falck (1996), some water at equilibrium with calcite CaCO_3 (pH 7.5) is transported by convection and dispersion in concrete (pH 12.5), leading to the dissolution of the portlandite $\text{Ca}(\text{OH})_2$. Once again, numerical results are in good agreement with previous results obtained from other reactive transport code (Read and Falck, 1996). In a second step, more complicated configurations have been simulated (Mügler et al., 2004). The code is now used to model and simulate real configurations of reactive transport. Among those, we focus here on two applications: the migration of uranium in a soil with various redox conditions and clay–cement interactions.

4. Migration of uranium in a soil with various redox conditions

Measurements performed in a polluted site with uraninite ($\text{UO}_{2(s)}$) have shown that the dissolved uranium concentration measured in a piezometer varies as a function of time: it increases in winter and decreases in summer according to variations of redox conditions and porewater composition (Descostes et al., 2005); soon available in (Phrommavanh et al., in preparation). Such variations are also observed with sulphur and nitrogen speciation: sulphide and ammonium ions are observed in summer, whereas thiosulphate, sulphate and nitrate ions are detected in winter, *i.e.*, under oxidizing conditions. Nitrate is known as a weak uranium complexing agent, whereas sulphur under thiosulfate and sulphate ions respectively can form uranium complexes, such as USO_4^{2+} , $\text{UO}_2\text{S}_2\text{O}_3$, UO_2SO_4 , $\text{U}(\text{SO}_4)_2$, $\text{UO}_2(\text{SO}_4)_2^{2+}$, $\text{UO}_2(\text{SO}_4)_3^{3-}$. These sulphonyanions are therefore liable to increase the solubility of uraninite. However sulphur and nitrogen can be also considered as redox tracers. A preliminary analysis suggests that dissolved oxygen ($\text{O}_{2(aq)}$) is highly suspected to diffuse in water saturated soils according to the maximum of precipitation observed in winter. A first attempt to understand the observed variations of redox conditions was achieved, considering an infiltration into the soil of a porewater equilibrated with atmospheric oxygen. This study is focusing on different redox systems, *i.e.*, uranium, nitrogen and sulphur speciation, which to our knowledge, is rarely taken into account or validated in geochemical modelling.

4.1. Methods

The numerical platform ALLIANCES has been used to model and simulate the site. In the simulation, water at

equilibrium with the oxygen atmosphere infiltrates a sub-surface aquifer with a 2.5 m/year constant vertical flow velocity, and leaches a zone enriched in three different uraninite subsystems. The studied system is presented in Fig. 1. Two different layers are considered: the soil, beginning from the surface down to a depth of 7.5 m, and underneath, the aquifer from 7.5 to 20 m. The simulated porous medium is a 600-element mesh bi-dimensional system (see Fig. 2). Additional modellings were performed with a refined mesh made of 2400 cells to improve the results. All subsystems have the same porosity (equal to 0.5) but have different initial chemical compositions. Kinematic dispersion is equal to 1.5 m everywhere. Initial chemical compositions of the soil and of the aquifer are different, with high contents of sulphide and ammonium in underground porewater, according to field data. Several simulations have been performed with an increasing complexity for the soil geochemistry with or without uranium (see Table 1). An inert tracer was first used to validate the transport modelling. All calculations were performed in NaCl 10^{-3} M media, in order to keep a constant ionic strength. We observe the evolution in time and space in the aquifer of aqueous speciation, elementary concentrations, but also Eh and pH. Modelling was achieved using a consistent thermodynamic data basis (Guillaumont et al., 2003), without considering any kinetic law.

4.2. Results

In order to see and calculate the penetration depth of dissolved oxygen, an inert tracer taken as tritiated water (HTO) is also injected from the surface (see Fig. 3 for example). All the treated cases are not presented, but the most relevant are discussed. When ammonium and/or

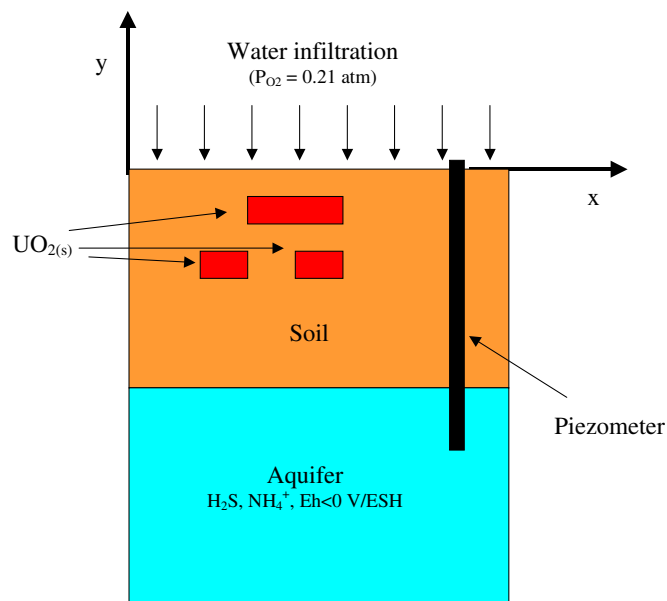


Fig. 1. Schematic representation of the studied polluted site.

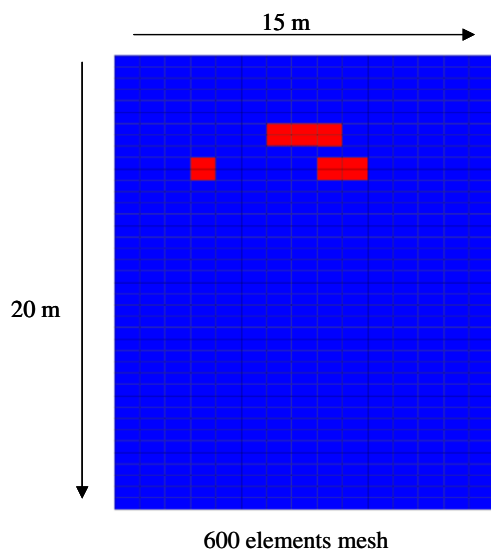
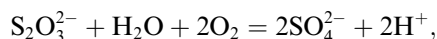
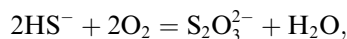


Fig. 2. Simulated porous media geometry.

sulphide ions are initially present, the oxygen is instantaneously consumed by the nitrate producing reaction, thio-sulfate and sulfate ions. These oxidation reactions are accompanied by an acidification according to



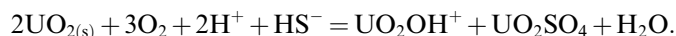
and



When ammonium and sulphide ions are both initially present, sulphur first reacts with oxygen to form thiosulfate and

sulfate, but also leads to the presence of two distinct Eh zones. Thiosulfate ions are metastable and their concentration remains very low (10^{-9} mol/L). This first modelling allows us to consider therefore more complex calculations with the simultaneous presence of different redox couples and uranium.

When only uranium is considered in the modelling (case 1 in Table 1), maximum uranium concentration is close to 10^{-7} mol/L, that is to say the solubility of schoepite (see Fig. 4). The main aqueous species are UO_2OH^+ and $\text{UO}_2(\text{OH})_2$ (see Fig. 5a). Schoepite is observed in the uraninite zones. In a more complex case (case 6 in Table 1), when nitrogen and sulphur are taken into account, the maximum uranium content increases to 10^{-5} mol/L. The speciation is modified since one of the predominant species is UO_2SO_4 (see Fig. 5b), according to the following overall reaction:



The other electroactive species oxidation is still taking place. Sulphide and nitrogen are respectively oxidized into thiosulfate, sulphate and nitrate.

The dissymmetry of the uranium concentration which appears in Fig. 4c and d is due to the dissymmetry of the initial conditions (see Fig. 2). Simulations presented in this paper have been performed with a 600-cell mesh. Simulations of the same configurations were performed with a refined mesh made of 2400 cells (2 times as many cells in each direction). Fig. 6a and b give the total concentration of uranium after 1 and 2 years, calculated with the refined mesh in the configuration number 6 described in Table 1. These figures have to be compared with Fig. 4c and d and check the spatial convergence of the numerical scheme.

Table 1
Different cases studied with or without the formation of $\text{S}_2\text{O}_3^{2-}$ and uraninite ('-' stands for not fixed, while $\text{UO}_{2(\text{s})}$ is defined by a concentration of $[\text{UO}_{2(\text{s})}] = 1 \text{ mol L}^{-1}$)

Case		pH	Eh (V/SHE)	P(O ₂) (atm)	[NH ₄ ⁺] (mol L ⁻¹)	[HS ⁻] (mol L ⁻¹)	[SO ₄ ²⁻] (mol L ⁻¹)
1	Soil	6.7	-0.1435	0	0	0	0
	Aquifer	7	-0.180	0	0	0	0
	Infiltration	-	-	0.2	0	0	0
2	Soil	6.7	-0.1435	0	10^{-4}	0	0
	Aquifer	7	-0.180	0	10^{-5}	0	0
	Infiltration	-	-	0.2	0	0	0
3	Soil	7	-	0	0	3×10^{-5}	6.93×10^{-3}
	Aquifer	7	-0.180	0	0	0	1.77×10^{-4}
	Infiltration	-	-	0.2	0	0	0
4	Soil	7	-	0	0	3×10^5	6.93×10^{-3}
	Aquifer	7	-0.230	0	0	-	1.62×10^{-4}
	Infiltration	-	-	0.2	0	0	0
5	Soil	7	-	0	10^{-4}	3×10^{-5}	6.93×10^{-3}
	Aquifer	7	-0.230	0	0	0	1.77×10^{-4}
	Infiltration	-	-	0.2	0	0	0
6	Soil	7	-	0	10^{-4}	3×10^{-5}	6.93×10^{-3}
	Aquifer	7	-0.180	0	0	-	1.77×10^{-4}
	Infiltration	-	-	0.2	0	0	0

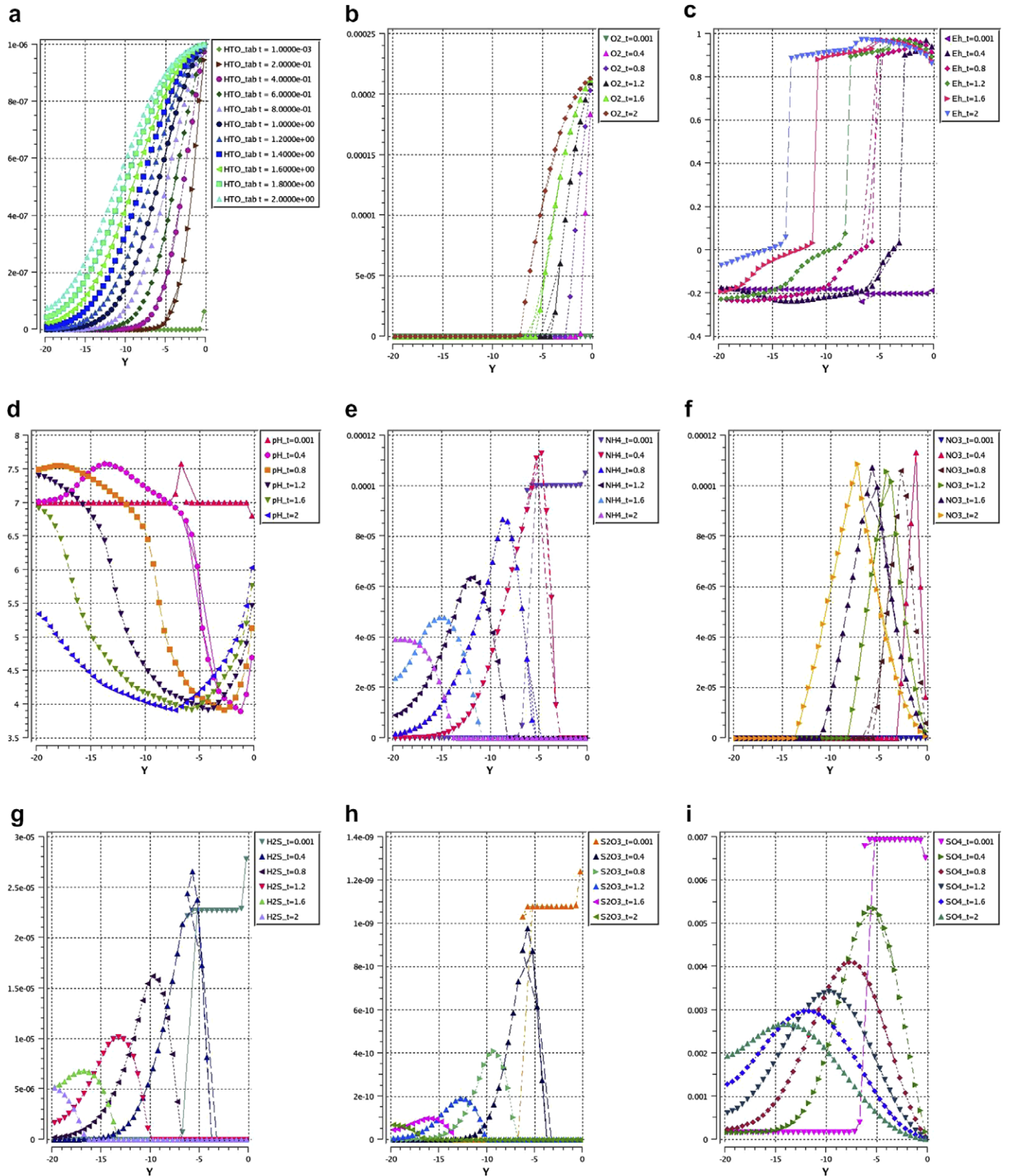


Fig. 3. Illustration of results obtained from the case 6 in Table 1, without uranium. Figures give vertical profiles at $x = 7.5$ m of the different species concentration (in mol/L), pH and Eh (in V/SHE), at different times: $t = 0.001, 0.4, 0.8, 1.2, 1.6$ and 2 years. ((a) HTO chosen as an inert tracer, (b) $[O_{2(aq)}]$, (c) Eh, (d) pH, (e) $[NH_4^+]$, (f) $[NO_3^-]$, (g) $[H_2S]$, (h) $[S_2O_3^{2-}]$, (i) $[SO_4^{2-}]$).

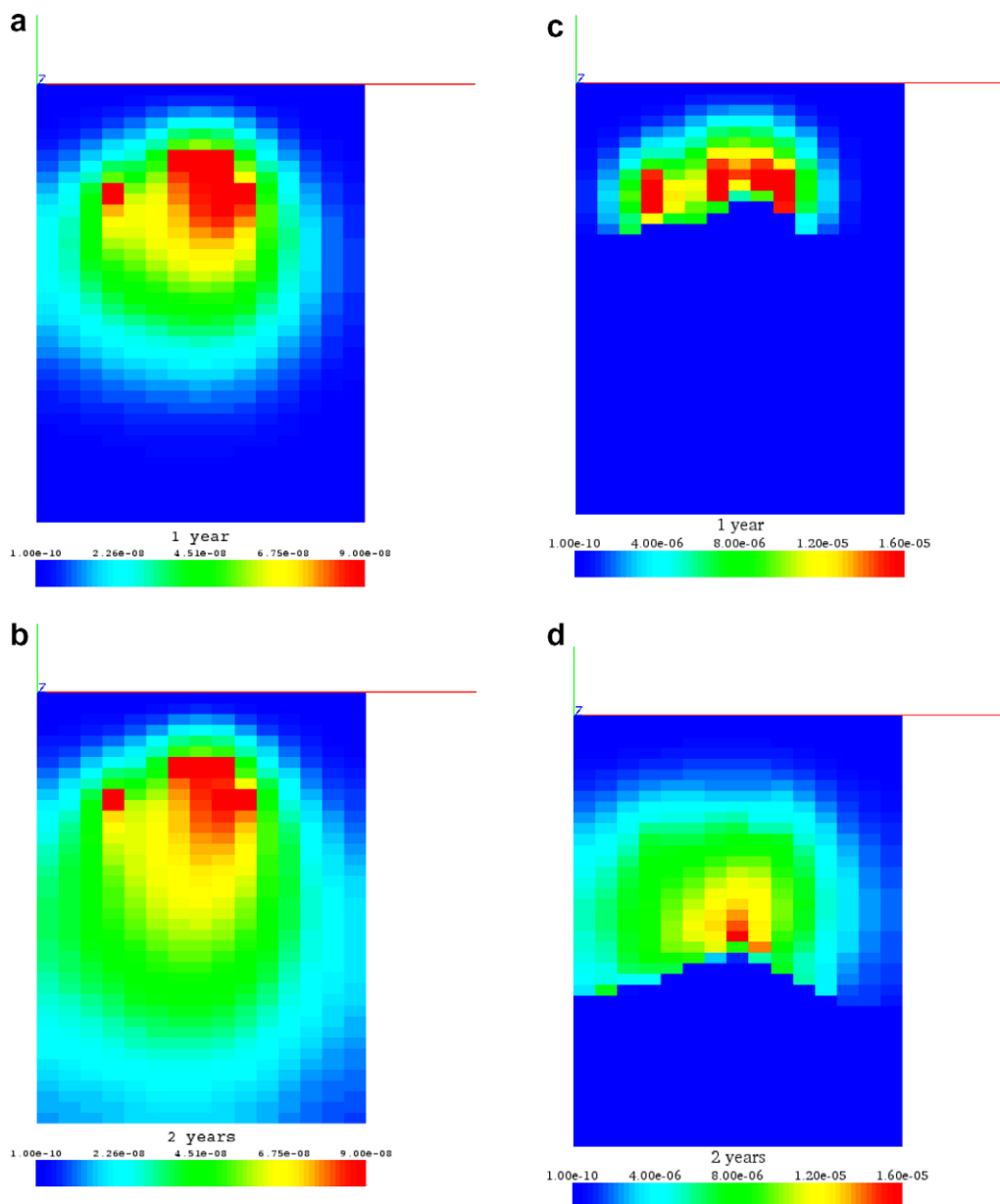


Fig. 4. Total concentration of uranium (mol/L) calculated at 1 year and 2 years, without (a) and (b) and with nitrogen and sulphur (c) and (d). Modellings without and with nitrogen and sulphur correspond to case 1 and case 6 in Table 1, respectively.

4.3. Discussion and perspectives

Several simulations have been performed with an increasing complexity for the soil geochemistry, including nitrogen and sulphur aqueous redox chemistry. Modelling shows the dissolution of $\text{UO}_{2(s)}$ and the subsequent uranium migration. When SO_4^{2-} but also $\text{S}_2\text{O}_3^{2-}$ are taken into account, the $\text{UO}_{2(s)}$ solubility increases due to the formation of $\text{S}_x\text{O}_y\text{-U}$ aqueous complex. Numerical results are in qualitative agreement with experimental measurements and show the interest of the use of a coupled reactive transport code. Moreover, one specific problem encountered in geochemical modelling, *i.e.*, redox behaviour, was resolved considering up to four different elements, with more than nine oxidation numbers.

This study prefigures a more complex and realistic configuration where a whole set of geochemical data will be considered. Thiosulfate ions are known to be metastable in natural environment (Descostes et al., 2002). Other inorganic complexing agents of both $\text{U}^{(\text{VI})}$ and $\text{U}^{(\text{IV})}$ such as sulfite (SO_3^{2-}) (Vitorge et al., submitted for publication) but also carbonate will be considered. We will focus on the equilibrium with carbonate minerals and the regulation of the CO_2 partial pressure in natural environment. Sorption properties of the soil delimited by clayey materials and pyrite (Eglizaud et al., accepted for publication) will be also considered. Physical properties of each layer, *i.e.*, porosity, permeability and kinematic dispersion, will be studied as coupled phenomena. Finally, boundary conditions will be

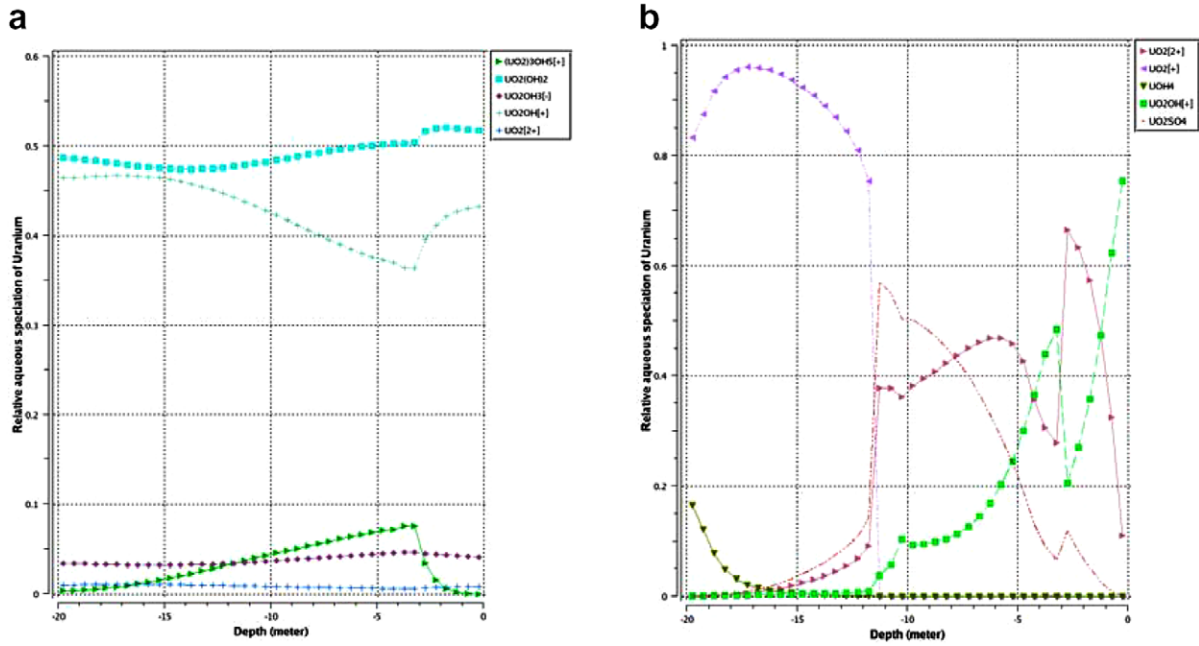


Fig. 5. Vertical profiles of relative aqueous speciation of uranium, at $x = 7.5$ m and $t = 2$ years, (a) without and (b) with nitrogen and sulphur. Modellings without and with nitrogen and sulphur correspond to case 1 and case 6 in Table 1, respectively. To make the figure clearer, only uranium main species are shown.

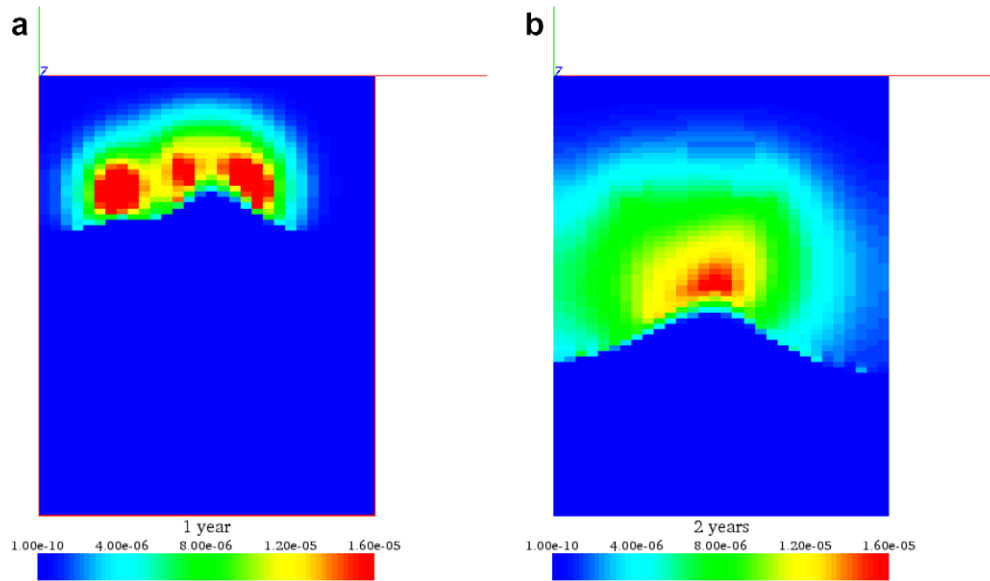


Fig. 6. The same as Fig. 4(c) and (d) but with a refined mesh made of 2400 cells.

modified in order to simulate the observed seasonal alternation of pluviometry.

5. Multidimensional modelling of clay–concrete interactions using ALLIANCES

In the context of geological disposal of nuclear waste, safety studies have to consider time scales accounting for the long period of the high-level and long living radionuclides. Moreover, safety assessments involve various phe-

nomena, which are often interdependent. However, time scales of laboratory experiments are necessarily short compared to repository ones and experiments are often focused on only one specific phenomenon (Jacquot and Michau, 2005). The first step of the modelling approach was to acquire experimental data on clay–concrete systems in order to assess mineral transformations of clayey materials under alkaline conditions. This has been done by various laboratory experiments (Rousell, 2001) as well as the study of natural analogues (Rassineux, 2001; Techer et al., 2004).

It was demonstrated that the phases observed in laboratory experiments are of the same nature as those observed on natural analogues, validating the fact that dissolved and precipitated phases observed in short term laboratory experiments are representative of longer time scales of interactions.

The second step consisted in checking that the numerical modelling of clay–concrete systems was consistent with phase transformations identified both experimentally and on the natural analogue sites. Hence, from the geochemical point of view, our modelling approach aim is to be representative of what is observed but not to be predictive by itself.

The third step consisted in coupling transport phenomena to the identified geochemical processes. Considering diffusion as the dominating transport process in clayey materials, the modelling developed in this study allowed us to estimate the propagation of an alkaline plume in time and space in the context of a geological disposal.

One dimensional coupled geochemistry-transport tools, such as PHREEQC, were beforehand used to give a rough estimation of the propagation of an alkaline plume in clayey systems. The main limitation of one dimensional transport is that the storage geometry can not be taken into account. Such difficulties can be overcome by the use of the ALLIANCES multidimensional coupling tool.

Hereafter we present numerical results associated to the simulation of a gallery sealing concept which involves bentonite, argilite and concrete areas whose interface evolution has to be evaluated over time. The driving force for the evolution of the system results from the chemical heterogeneity between each material and in particular between the concrete and the argillaceous materials. The interstitial fluid pH for the concrete is estimated at 12.4 whereas the bentonite and the argillite ones are respectively 7.8 and 7.0. The geometry of the concept is represented in Fig. 7 together with the boundary conditions taken for the numerical modelling. In this figure, one can notice a small bentonite zone embedded in concrete that we call thereafter bentonite key. The extension of the argilite is of 60 meters. Transport parameters are listed in Table 2 where the EDZ corresponds to a damaged zone of the argilite due to excavation. The mineral composition of each material is described in Tables 3–5. In the simulation, Feldspar and Pyrite are not supposed to precipitate due to the low temperature considered (25 °C).

Results presented thereafter have been obtained within ALLIANCES with the PHREEQC/MT3D coupling over a 1500-element mesh. Only diffusive transport is considered enabling to take symmetry axes into account. Alteration over time of the concrete occurs only at interfaces with clayey materials where Portlandite is dissolved (see Fig. 8) and new minerals, as low Ca/Si ratio CSH, appear (see Fig. 9). For the bentonite key, only cation exchange is stated, Na-Montmorillonite being replaced by Ca-Montmorillonite whereas at the bentonite/concrete interface, both Montmorillonite are dissolved (see Figs. 10 and 11).

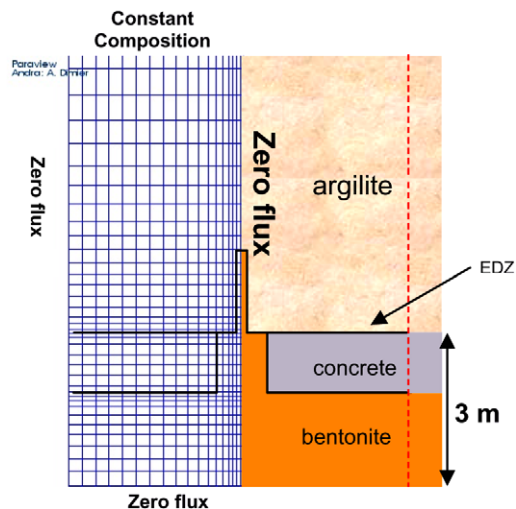


Fig. 7. Representation of the geometry near the concrete/bentonite interface and associated meshing considered.

Table 2
Clay–concrete interactions: transport parameters associated to the materials or zones

Zones	Effective diffusion
Bentonite	10^{-11} m ² /s
Argilite	2.6×10^{-11} m ² /s
Concrete	10^{-11} m ² /s
EDZ	5.2×10^{-11} m ² /s

Table 3
Clay–concrete interactions

Phase	Amount (mol/kg w)
Portlandite	16.05
CSH 1.65	7.50
Hydrogrenat	1.11
Hydrotalcite	0.32
Ferrihydrite	0
Monosulfoaluminate	0.96
Pyrite	1.47
Calcite	195.71

Mineral composition of Concrete.

Table 4
Clay–concrete interactions

Phase	Amount (mol/kg w)
Quartz	57.97
K-Feldspar	2.40
Calcite	25.33
Dolomite	6.60
Célestine	0.64
Pyrite	2.36
Illite	12.30
Ca-Montmorillonite	6.63
Daphnite	0.26
Chlorite-14A	0.26

Mineral composition of Argilite.

Table 5
Clay–concrete interactions

Phase	Amount (mol/kg w)
Montmorillonite-Na	4.60
Montmorillonite-Ca	4.61
Biotite-Fe	0.22
Pyrite	0.10
Calcite	0.39
Albite	0.53
K-Feldspar	0.15
Quartz	4.68

Mineral composition of Bentonite.

On the argilite side, dissolution of the initially present Ca-Montmorillonite is observed (see Fig. 10). Simulations show the permanence of a bentonite zone over time in spite of its interaction with an alkaline plume.

6. Conclusion

A coupled transport/chemistry simulation tool has been developed in the context of the software platform ALLI-ANCES. It has been validated against many configurations and is now successfully used to model and simulate real configurations of reactive transport.

We focus here on two applications of the code. The first one deals with the migration of uranium in a soil with various redox conditions. Numerical results are in qualitative agreement with experimental measurements and show the interest of the use of a coupled reactive transport code. Moreover, one specific problem encountered in geochemical modelling, *i.e.*, redox behaviour, was resolved considering up to four different chemical elements, with more than nine oxidation numbers. The second application of the code deals with the modelling of clay–cement interactions.

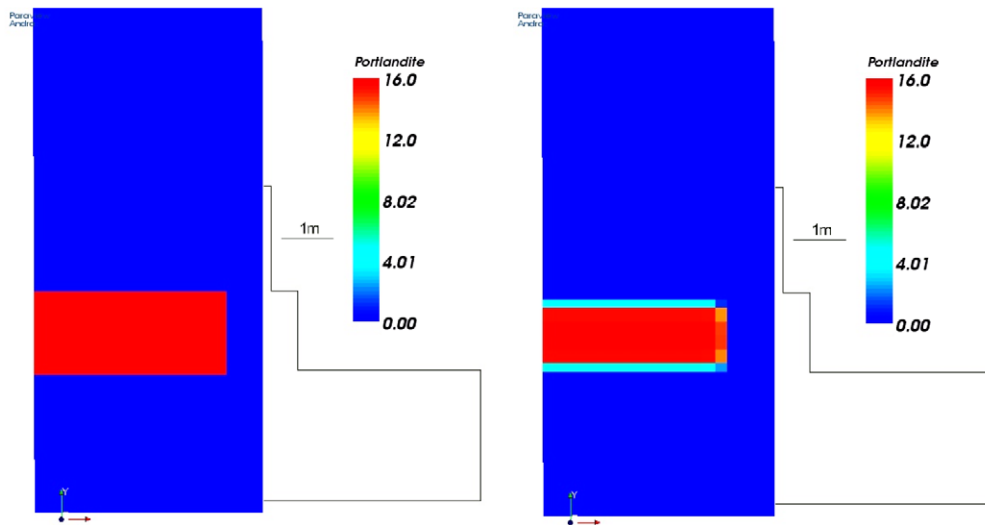


Fig. 8. Portlandite amount mol/kg w, initially and after 100 000 years.

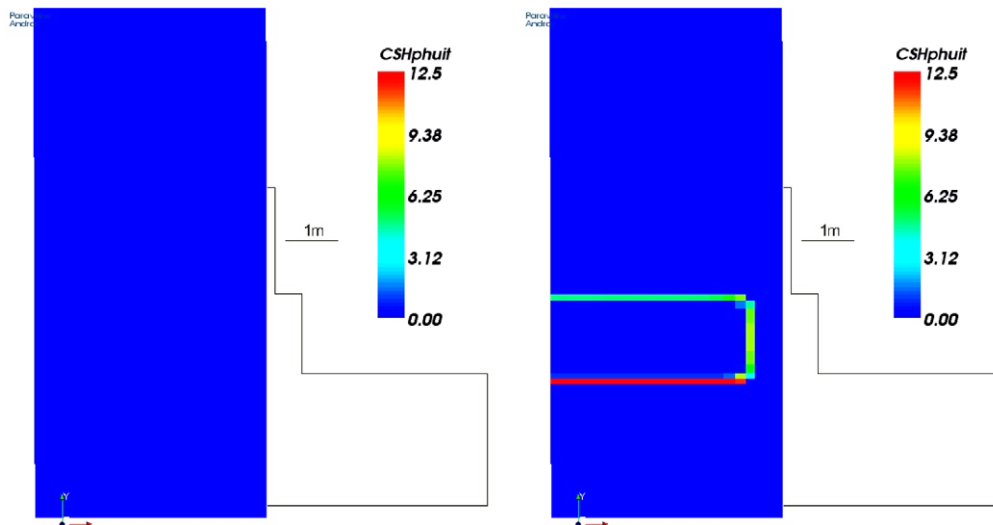


Fig. 9. CSH_0.8 amount mol/kg w, initially and after 100 000 years.

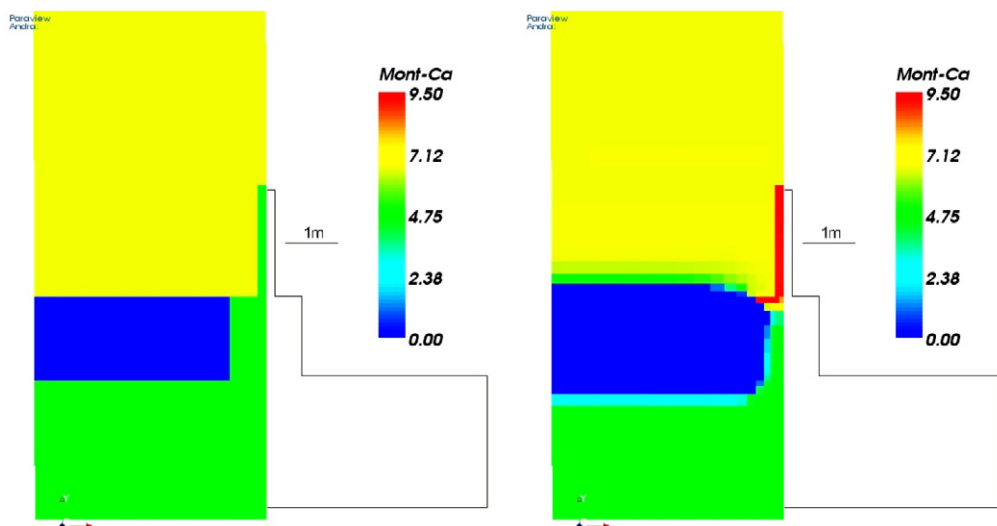


Fig. 10. Montmorillonite Ca amount mol/kg w, initially and after 100 000 years.

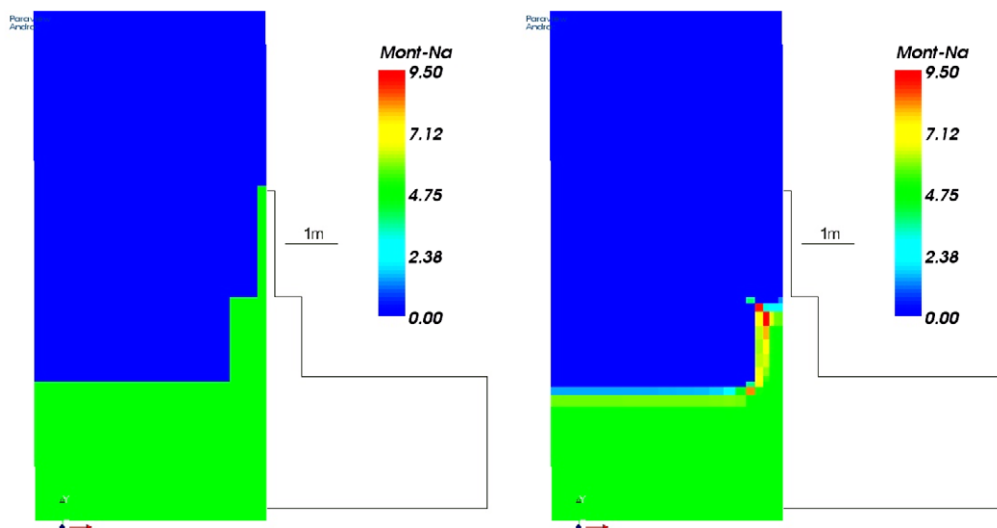


Fig. 11. Montmorillonite Na amount mol/kg w, initially and after 100 000 years.

Simulations show the permanence of a bentonite zone over time in spite of its interaction with an alkaline plume. These two studies show the interest of the use of a multidimensional coupled reactive transport code in order to interpret long term behaviour of a nuclear waste disposal or polluted site.

To go further in the simulation, we will take unsaturated media (for subsurface simulations or saturation/desaturation scenarios) into account. Therefore, next version of ALLIANCES will include chemistry-transport coupling with unsaturated flows.

References

- Bernard-Michel, G., Le Potier, C., Beccantini, A., Chrebi, M., 2003. The ANDRA Couplex 1 test-case: comparisons between finite element, mixed-hybrid-finite element and finite volume discretizations with CAST3M. *J. Comput. Geosci.* 8, 187–201.
- Dabbene, F., 1998. mixed-hybrid finite elements for transport of pollutants by underground water. In: *Proc. of the 10th Int. Conf. on Finite Elements in Fluids*, Tucson, USA.
- Descostes, M., Beaucaire, C., Mercier, F., Savoye, S., Sow, J., Zuddas, P., 2002. Effect of carbonate ions on pyrite (FeS_2) dissolution. *Bulletin de la Société Géologique de France* 173, 265.
- Descostes, M., Mügler, C., Montarnal, P., Colin, J., Phommavanh, V., 2005. Modelling uranium migration in different redox conditions (with ALLIANCES reactive-transport module), *MIGRATION'05*, Avignon, France.
- Eglizaud, N., Miserque, F., Simoni, E., Schlegel, M., Descostes, M., accepted for publication. Uranium (VI) interaction with pyrite (FeS_2): chemical and spectroscopic studies, to appear in *Radiochimica Acta*.
- Guillaumont, R., et al., 2003. Update on the Chemical Thermodynamics of Uranium, Neptunium, Plutonium, Americium and Technetium. NEA-TDB, OECD, Amsterdam.
- Jacquot, E., Michau, N., 2005. La perturbation alcaline liée à un stockage: les argilites du Callovo-Oxfordien en champ proche et les composants à base d'argile gonflante. Site de Meuse/Haute-Marne. Rapport Andra No. C.NT.ASTR.03.069.

- Montarnal, P., Bengaouer, A., Chavant, C., Loth, L., 2006. ALLIANCES: Simulation platform for nuclear waste disposal. In: Proc. of CMWR'06, Copenhagen, Denmark.
- Mügler, C., Montarnal, P., Dimier, A., Trotignon, L., 2004. Reactive transport modelling on the ALLIANCES software platform. In: Proc. of the 15th Int. Conf. on Computational Methods in Water Resources, Chapel Hill, NC, USA.
- Parkhurst, D.L., Appelo, C.A.J., 1999. User's guide to PhreeqC, version 2, Water-Resources Investigations Report 99.
- Phrommavanh, V., Descostes, M., Beaucaire, C., Gaudet, J.P., in preparation. Uranium migration in peatland: geochemical characterization.
- Rassineux, F. 2001. Projet Maqarin phase IV. Contribution à l'identification des transformations minéralogiques de la biomicrosite au contact de solutions alcalines sur le site de Khushaym Matruk. Document ANDRA D.RP.0ERM.01.019.
- Read, D., Falck, W. 1996. CHEMVAL 2: a coordinated research initiative for evaluating and enhancing chemical models in radiological risk assessment, vol. EUR 16648-EN of Nuclear Science and Technology EC Series.
- Rousell, 2001. Etude expérimentale et modélisation de la propagation d'une onde de concentration alcaline issue d'une matrice cimentière à travers l'argilite du site du laboratoire de Meuse/Haute-Marne. Thèse de l'Institut National Polytechnique de Lorraine, Nancy 1, 212 p.
- Techer, I., Fourcade, S., Elie, M., Martinez, L., Boulvais, P., Claude, C., Clauer, N., Pagel, M., Hamelin, B., Lancelot, J. 2004. Contribution des analogues naturels à la compréhension du comportement à long terme des milieux argileux vis-à-vis de la circulation de fluides hyperalcalins: Etude du site de Khushaym Matruk en Jordanie Centrale; Géochimie isotopique du Sr, du C et de l'O; Datations U-Th, K-Ar; Caractérisation de la matière organique. Rapport final du GdR FORPRO. Action de recherche 2001-VII.
- van der Lee, J., de Windt, L., 2002. Chess Tutorial and Cookbook, updated for version 3.0, ENSMP-CIG LHM/RD/02/13.
- Vitorge, P., Phrommavanh, V., Siboulet, B., You, D., Vercouter, T., Descostes, M., Marsden, C.J., Beaucaire, C., Gaudet J.P., submitted for publication. Estimating the stabilities of actinide aqueous species. Influence of sulfoxy-anions on uranium (IV) geochemistry. C.R. Acad. Sci.
- Yeh, G.T., Tripathi, V.S., 1989. A critical evaluation of recent developments in hydrogeochemical transport models of reactive multichemical components. *Water Resour. Res.* 25, 93.
- Zheng and Wang, 1998. MT3DMS Documentation and User's Guide.